

Research Article



Molecular Recognition

How to cite: Angew. Chem. Int. Ed. 2024, e202408751 doi.org/10.1002/anie.202408751

Tailoring Metallosupramolecular Glycoassemblies for Enhancing Lectin Recognition

Julia M. Stauber*

Abstract: Multivalency is a fundamental principle in nature that leads to high-affinity intermolecular recognition through multiple cooperative interactions that overcome the weak binding of individual constituents. For example, multivalency plays a critical role in lectincarbohydrate interactions that participate in many essential biological processes. Designing high-affinity multivalent glycoconjugates that engage lectins results in systems with the potential to disrupt these biological processes, offering promising applications in therapeutic design and bioengineering. Here, a versatile and tunable synthetic platform for the synthesis of metallosupramolecular glycoassemblies is presented that leverages subcomponent self-assembly, which employs metal ion templates to generate complex supramolecular architectures from simple precursors in one pot. Through ligand design, this approach provides precise control over molecular parameters such as size, shape, flexibility, valency, and charge, which afforded a diverse family of well-defined hybrid glyconanoassemblies. Evaluation of these complexes as multivalent binders to Concanavalin A (Con A) by isothermal titration calorimetry (ITC) demonstrates the optimal saccharide tether length and the effect of electrostatics on protein affinity, revealing insights into the impact of synthetic design on molecular recognition. The presented studies offer an enhanced understanding of structure-function relationships governing lectin-saccharide interactions at the molecular level and guide a systematic approach towards optimizing glyconanoassembly binding parameters.

Introduction

Carbohydrates present an important class among the natural building blocks of biopolymers as glycan-protein interactions participate in many essential biological processes

[*] Prof. Dr. J. M. Stauber Department of Chemistry and Biochemistry University of California, La Jolla, 92092 San Diego, California, United States E-mail: jstauber@ucsd.edu

© 2024 The Authors. Angewandte Chemie International Edition published by Wiley-VCH GmbH. This is an open access article under the terms of the Creative Commons Attribution License, which permits use, distribution and reproduction in any medium, provided the original work is properly cited.

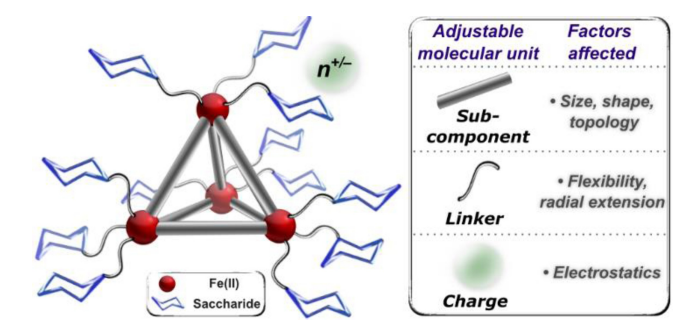


Figure 1. Structure of metallosupramolecular core displaying the adjustable design parameters examined in this work.

including immune function, cell-signaling, the recognition of pathogens, among others.^[1,2] The spatial and topological presentation of carbohydrates in naturally-occurring glycomacromolecules provides the underlying keys for specific and high affinity biomolecular recognition events that occur through simultaneous strong, yet reversible multivalent binding. Multivalency is a fundamental principle in nature that leads to high binding avidity and selectivity in which multiple, cooperative receptor-ligand recognition events the comparatively enhance weaker individual interactions.^[3-5] Given the diverse roles that multivalent protein-carbohydrate interactions play in human health, there has been intense interest in developing saccharidegrafted synthetic assemblies that probe these interactions due to the wide-ranging potential utility of such systems in therapeutic applications.^[5–8]

Multivalent glycan assemblies are typically constructed around a central core that is covalently linked to multiple carbohydrate epitopes decorating the molecular periphery. [9] A variety of scaffolds have been used for these systems including small organic and inorganic molecules, [10-13] dendrimers, [14,15] polymers, [16-18] peptides, [19] nucleic acids, [20,21] nanoparticles, [22] among others (Figure 1). [23-25] Despite ongoing interest in developing such classes of hybrid glycoconjugates, structurally well-defined cluster assemblies remain relatively rare, [26-31] and methods of systematically optimizing and regulating recognition behavior in existing molecular frameworks are limited. This scarcity poses challenges in mimicking naturally occurring biomolecular recognition events from a fundamental structure-activity perspective, as nature achieves high levels of control, selectivity, and affinity through principles including substrate cooperativity and structural preorganization. Nevertheless, advancing the fundamental understanding of these



intricate biological recognition events requires the continued development of synthetic assemblies that resemble both the structural and functional complexity inherent in nature.

Subcomponent self-assembly is a powerful synthetic strategy that has been leveraged to build complex and architecturally well-organized structures from simple building blocks that is reminiscent of the way nature generates many multi-component supramolecular assemblies.[32-34] Coordination-driven subcomponent self-assembly utilizes molecular synthons and non-covalent interactions to direct the formation of more complex systems while maintaining the same degree of predictability and control attainable in molecular synthesis. [35,36] In recent years, metallosupramolecular chemistry has undergone rapid development due to its catalysis,[32,37-39] wide-ranging applications in bionanotechnology, [40-42] molecular sensing, [43] reactive species stabilization, [44-47] among many others. [48,49] Metallosupramolecular assemblies have most commonly been exploited for their host-guest chemistry; however, this work leverages such systems as synthons for the preparation of multivalent biomolecular architectures through surface functionalization, merging synthetic supramolecular chemistry with biomolecular recognition. Recently, we demonstrated the modularity, tunability, and versatility of coordinationdriven subcomponent self-assembly in the synthesis of structurally well-defined iminopyridine-supported glycomolecules that show strong multivalent binding to a lectin target.^[50] This supramolecular approach allowed for rational synthetic control over glycoassembly multivalent binding behavior and enabled a systematic method of building precision nanomolecules that are programmable in terms of their size, shape, topology, saccharide surface density, and valency. This platform holds notable advantages over other classes of multivalent molecular systems due to the operational simplicity of the synthetic approach and the interchangeable nature of the constituent building blocks, which offer high potential for systematic and rapid diversification of molecular architectures.

In this work, the supramolecular landscape is expanded by introducing modifications to the ligand design that specifically impact the flexibility, radial extension, electrostatics, and size of the resulting assemblies (Figure 1). Here, we present a new generation of glycan-tethered pyridyl building blocks bearing flexible chains of systematically varied length that are paired with two benzidine-based ditopic amines. In the presence of Fe(II), this combination of subcomponents afforded two series of tetrahedral glycoassemblies bearing M₄L₆ core structures first introduced by Nitschke et al. (M=metal, L=ligand). [44,51] We further introduce an isocyanurate-based tritopic amine subcomponent that produced a series of face-capped Fe₄L₄ complexes, thus increasing the diversity of glycomolecules in this study with a new metal-organic polyhedral core. The complexes were evaluated as multivalent binders to the lectin Concanavalin A (Con A), and results from the binding analyses demonstrate the impact of rational synthetic design on the strength of the molecular recognition events. This study illustrates that a versatile synthetic platform can offer valuable insights into factors governing structure function

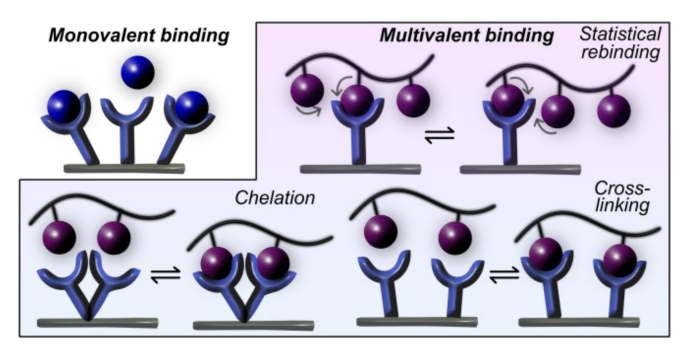


Figure 2. Monovalent binding representation and mechanisms of interaction between multivalent ligands and multivalent receptors. Statistical rebinding and cross-linking represent plausible binding mechanisms of multivalent binders described in this study with Con A, while a chelation mechanism occurs when the size of the glycoassembly is sufficiently large to bridge binding sites. Spheres are a general representation of glycan units on multivalent binders.

relationships and provides a rational approach to the optimization of binding parameters.

Results and Discussion

Subcomponent Design

When paired with α-mannose-functionalized picolinaldehyde, e, amine building blocks proved to be excellent reaction partners that enabled the preparation of a series of monodisperse tri-, hexa-, and dodecavalent ($[1e]^{4-}$, Scheme 1) Fe(II)-anchored glycan assemblies, as previously reported.^[50] This synthetic method proceeds through the formation of both coordinative $N{\rightarrow}M$ and covalent $C{=}N$ linkages to result in supramolecular complexes supported by pyridylimine ligand backbones that demonstrate high stability and solubility in aqueous media. $^{[44,52,53]}$

The present study was initiated by methodically evaluating the effect of saccharide topological display on protein binding efficiency by modulating the carbohydrate linking units. Poly(ethyleneglycol) (PEG) groups are widely employed as spacer arms in the design of multivalent glycoconjugates to link terminal saccharides to assembly cores.[10,54,55] PEG is a hydrophilic, nontoxic polymer that does not promote immune responses, and has consequently played an indispensable role in pharmaceutical applications. [56] In the context of this work, ethyleneglycol (EG) groups have the potential to impart valuable functional benefits to supramolecular glycoassemblies including exceptional water solubility and versatility in terms of chain length. The presence of an alcohol group amenable to direct use in glycosidic bond formation also provides synthetic utility and the EG C-O linkages impart significant flexibility, offering a high range of movement for peripherally linked saccharides. While assemblies featuring rigid spacers can achieve more effective binding than assemblies with flexible frameworks due to lower entropic loss upon chelation, their design can be more challenging as they

5213773, Q. Downloaded from https://onlinelibrary.wiley.com/doi/10.1002/anie.202408751 by University Of California, Wiley Online Library on [17/09/2024]. See the Terms and Conditions (https://onlinelibrary.wiley.com/terms-and-conditions) on Wiley Online Library for rules of use; OA articles are governed by the applicable Creative Commons. License

Scheme 1. Synthetic Schemes for the preparation of picolinal dehyde glycan subcomponents e-f (top), and Fe(II) glycoassemblies [1 e-h]⁴⁻, [2 e h_1^{8+} , and $[3e-h_1^{8+}]$ (bottom). Reaction conditions: A: BF₃·(Et₂O), ZnCl₂ (cat), CH₂Cl₂, 16 h, 25 °C; B: K₂CO₃, dimethylformamide, 70 °C, 16 h; C: NaOMe (cat), MeOH, 25 °C, 16 h.

require a perfect fit with their protein binding partner. [57] The integration of EG linkers in molecular design, however, enhances flexibility, which can potentially enable easier access to protein binding pockets while also facilitating important statistical rebinding, cross-linking and chelate events that promote stronger interactions with multivalent receptors (Figure 2).^[58]

As shown in Scheme 1, the linker lengths connecting α-mannose units to the iminopyridine ligand framework were systematically varied by incorporating mono-, [50] di-, tri-, and tetraethyleneglycol groups at the 5-position of the formyl pyridine subunit through conversion of the parent diols to the mono-brominated derivatives. These linkages were then tethered to the anomeric position of tetraacetateprotected α-D-mannose through Lewis-acid assisted O-glycosylation. The glycan building blocks were easily coupled to 5-hydroxypicolinaldehyde in the presence of K₂CO₃ to afford the mannosylated picolinal dehyde subcomponents (a-d) after purification by flash liquid chromatography. Quantitative de-O-acetylation under standard Zemplén conditions (NaOMe, MeOH)[59] afforded the deprotected α-mannopyranoside congeners, e-h, after neutralization using the acidic Amberlyst -15 ion-exchange resin. The deprotected subcomponents were then used in self-assembly reactions without subsequent purification. However, the per-O-acetylated forms, a-d, also proved suitable for direct use in self-assembly reactions upon in situ de-O-acetylation with stoichiometric hydroxide ion (See Supporting Information for experimental details).

With this family of systematically extended mannosylated building blocks in hand, synthetic investigations began by pairing diethyleneglycol-linked subcomponent, f, with benzidine sulfonic acid in the presence of $Fe(BF_4)_2 \cdot 6H_2O$. After precipitation from the crude reaction mixture, the product was easily separated away from low molecular weight byproducts via size-exclusion chromatography to afford the [NMe₄]₄[1f] salt in pure form. The purified product was characterized by ¹H nuclear magnetic resonance (NMR) spectroscopy, as displayed in Figure 3A. The spectroscopic data reveal a single set of well-defined resonances attributed to the iminopyridine ligand framework, suggesting the complex has idealized T-symmetry on the NMR timescale in solution. [60,61] The resonances lie exclusively within the diamagnetic region of the spectrum, demonstrating that the [1f]⁴⁻ anion contains all four Fe(II) centers in the low-spin, S=0 state. In line with successful imine condensation and complete consumption of subcomponent, f, the ¹H NMR spectrum of [NMe₄]₄[1f] is absent of an aldehyde resonance and exhibits a diagnostic imine signal located at δ 9.13 ppm (D₂O). Characterization of [NMe₄]₄[1f] by UV/Vis spectroscopy revealed metal-toligand charge transfer excitations centered at $\lambda = 505$ $(\epsilon 23,000 \,\mathrm{M}^{-1}\,\mathrm{cm}^{-1})$ and 545 $(\epsilon 26,000 \,\mathrm{M}^{-1}\,\mathrm{cm}^{-1})$ nm (Figure 3B), which are in line with low-spin Fe(II) in an

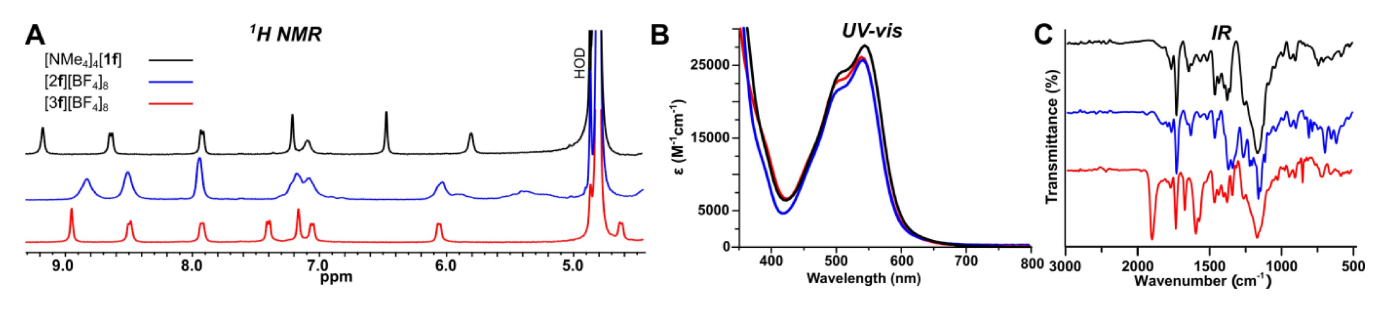


Figure 3. A: H NMR spectra of [NMe4]4[1 f], [2 f][BF4]8, and [3 f][BF4]8 (D2O, 25 °C). B: UV/Vis spectra of [NMe4]4[1 f], [2 f][BF4]8, and [3 f][BF4]8 (H2O, 50 μ M). C) ATR-IR spectra of [NMe₄]₄[1 f], [2 f][BF₄]₈, and [3 f][BF₄]₈.

iminopyridine coordination environment and consistent with data reported for similar systems.^[50,62,63] Infrared (IR) spectroscopy also supported the formation of an imine bond and coordination of the nitrogen donor atom to the Fe center as confirmed by the absence of an aldehyde vibration in the IR spectrum of [NMe₄]₄[1f] and the presence of a strong vibration ascribed to the imine C=N stretch (v_{C=N} 1558 cm⁻¹, Figure 3C). The identity of the product was unequivocally confirmed as the Fe4 tetrahedral cage grafted with twelve pendant mannosides by high-resolution electrospray mass spectrometry (ESI-MS(-), Supporting Information Figure S31).

Following the successful preparation of [NMe₄]₄[1f], the same methodology was applied to the systematic assembly of mannose-appended tetrahedral cages containing formylpyridine building blocks with longer EG chains. Accordingly, the tri- and tetraethylene glycol-linked derivatives, $[NMe_4]_4[1g]$ and $[NMe_4]_4[1h]$ respectively, were isolated and fully characterized by 1H NMR, UV/Vis, and IR spectroscopy. The identities of both species were established by HR-ESI-MS(-). The isolation of this series of supramolecular assemblies completes the family of anionic architectures presented in this study that feature flexible tethers connecting the rigid tetrametallic core to twelve appended carbohydrates.

Efforts were next centered on assembling cationic equivalents of complexes [1e-h]4- that retain the same mannose surface densities and spatial arrangements while maintaining uniformity in terms of the size and shape of the Fe₄ cage core. To this end, the 2,2'-bis(hydroxymethyl)benzidine ligand, 2, was selected as a neutral, ditopic, diamine building block that has previously been employed to prepare an iminopyridine-supported Fe4 tetrahedron. [51] As reported, this building block provides the resulting parent assembly with water stability and solubility on account of the twelve peripherally-located CH2OH groups.^[51] Importantly, incorporation of this subcomponent yields a neutral iminopyridine ligand and results in a nanoassembly that now carries an 8+ charge, which establishes a platform for the resulting mannose-decorated derivatives to serve as cationic analogues of their tetraanionic counterparts ([1e-h]⁴⁻, see above). In fact, structural determination of the parent 2'-bis(hydroxymethyl)benzidine-supported tetrahedron shows very similar Fe-Fe distances and Fe₄ core size when compared with the crystallographically-determined parameters of the benzidine sulfonate Fe₄ derivative. [64] These similarities suggest that the 2,2'-bis(hydroxymethyl)benzidine-supported glycoassemblies will closely mirror the size and shape of the [1e-h]4- complexes, underscoring that the primary distinction between the two series lies in their overall charge.

As subcomponent 1 proved to be an excellent building block for the straightforward self-assembly of complexes [1e-h]⁴⁻, the same synthetic approach was employed to prepare the octacationic, hydroxymethyl derivatives. The reaction of 2,2'-bis(hydroxymethyl)benzidine (6 equiv) with **e-h** (12 equiv) in the presence of $Fe(BF_4)_2 \cdot 6H_2O$ (4 equiv) in aqueous media under a nitrogen atmosphere led to conversion to the corresponding tetrahedral assemblies, $[2e-h]^{8+}$, under mild heating. The identities of all products were confirmed by high-resolution ESI-MS(+), revealing the presence of adducts composed of the octacationic species with charge compensating anions (See Supporting Information Section S2.2 for details). All products were also thoroughly characterized by 1H NMR, UV/Vis, and IR spectroscopy. The ¹H NMR spectra of all species in this series display broadened aryl signals in D₂O. These spectral features are ascribed to the presence of multiple conformers in solution due to restricted rotation around the central phenyl-phenyl bond caused by H-bonding interactions between the ortho-CH₂OH groups of the biphenyl framework. [65-67] Similar spectroscopic signatures have been reported for the parent, unfunctionalized Fe₄ tetrahedron, ^[51] and this behavior is typical for ortho-substituted biphenyl carbinols.[66]

To further expand the family of building blocks required for construction of a versatile library of glycosylated architectures, an additional neutral amine subcomponent that would provide access to a second series of octacationic complexes was selected. The triamine, tritopic subcomponent, tris(4-aminophenyl)isocyanurate (3), [68] was chosen due to its water-solubilizing polar groups that would enforce the required aqueous compatibility for this work when paired with a water-soluble Fe(II) salt.[69-71] In contrast to edge-linked tetrahedral assemblies of the form, M₄L₆, where ditopic ligands bridge two metal centers, tritopic ligands enforce a face-capped M₄L₄ motif where each ligand links three metal ions to establish the three-fold axis of symmetry of the structure. [60] Incorporation of this face-capping subcomponent increases the versatility of the glycoassem-



blies presented in this study by introducing structural diversity in terms of architectural size. It can be inferred that assemblies prepared from 3 would exhibit a core size larger than those of the $[1]^{4-}$ and $[2]^{8+}$ systems based on reported crystallographically determined parameters of Fe₄L₄ complexes derived from ligands of similar molecular footprint. [60]

Isocyanurate 3 was prepared in two synthetic steps via catalytic cyclotrimerization of 4-nitrophenylisocyanate followed by Clemmensen-type reduction to afford the triamine cyclotrimer. [68] Reaction of triamine 3 (4 equiv) with subcomponents **e-h** (12 equiv) and $Fe(BF_4)_2 \cdot 6H_2O$ (4 equiv) in a 2:1 H₂O/MeCN solvent mixture yielded tetrahedral cages [3e-h][BF₄]₈ after 16 h at 25 °C. The organic co-solvent was required in these syntheses to solubilize 3; however, once assembled, all products are water soluble. The ¹H NMR spectra of complexes [3e-h]8+ all feature one set of resonances, consistent with the formation of T-symmetric structures in solution in which all four iron centers of the tetrahedron adopt the same configuration. The set of [3e**h**][BF₄]₈ salts were also characterized by UV/Vis and IR spectroscopy, with spectroscopic signatures consistent with those described for the $[1e-h]^{4-}$ and $[2e-h]^{8+}$ analogues (see above). The identities of all cages were confirmed by HR-ESI-MS(+). Detailed characterization data of the series are presented in the Supporting Information, and Figure 3A-C displays the NMR, UV/Vis, and IR spectroscopic data for the [3f][BF₄]₈ assembly. As this work introduces isocyanurate 3 as a new subcomponent for Fe-anchored iminopyridyl metal organic polyhedra, the parent, unfunctionalized cage $([3][BF_4]_8)$ was also synthesized, and this complex is reported as a new, water-soluble Fe₄L₄ assembly (characterization data detailed in the Supporting Information Section S2.2.12).

Systematic Assessment of Lectin Binding Affinity

After demonstrating the synthetic scope of the developed chemistry, the impact of structural and electronic factors of the present systems to engage lectins using Con A as a model protein target was assessed. Con A is a plant lectin derived from jack bean (Canavalia ensiformis) seeds^[72] that specifically recognizes α-D-manno- and α-D-glucopyranosides. Con A is composed of 26 kDa monomeric units that each contain one saccharide binding site, and exists as a homodimer at pH < 6, a homotetramer at physiological pH, and as an equilibrium mixture of dimer and tetrameric forms at pH 6–7. [73] Con A is one of the most widely studied lectins in biological research owing to its structural resemblance to many animal and bacterial lectins, as well as its selectivity for saccharides commonly found in cellular glycoproteins and glycolipids.^[74] These properties have established Con A as an invaluable tool for probing lectin-carbohydrate interactions critical to diverse biological processes such as cell adhesion, cell signaling, and immune responses.^[75,76] The structure of Con A has also been well-established through crystallographic determination, [77] making it an excellent model for investigating protein-saccharide interactions at the molecular level.

In order to systematically investigate the thermodynamic binding parameters of the glycoassembly/Con A interactions in solution, isothermal titration calorimetry (ITC) was employed.^[73] Previous studies demonstrated that multivalent assemblies have a high propensity to form insoluble crosslinked aggregates with Con A in its tetrameric form, which consequently compromises the reliability of thermodynamic data (See Supporting Information Section S4.2 for protein agglutination studies). To circumvent this issue, all experiments in this study were performed at low protein concentration, low salt concentrations (NaCl, CaCl₂, MnCl₂), and in acidic conditions (pH 4.8), where Con A predominantly exists in its dimeric form.^[72] To confirm that no insoluble Con A cross-linked aggregates precipitate under the conditions used for the ITC experiments, turbidimetric studies were performed on selected assemblies examined in this study using UV/Vis spectroscopy, and additional experimental details can be found in the Supporting Information (Section S4.1).

As the separation between individual monomeric binding sites on Con A (ca. 8 nm)[78] precludes chelation of the dimeric lectin by the glycoassemblies (Figures 2 and 4), isotherm data were fitted using a single-site binding model based on monomeric Con A. Figure 5 displays thermograms and integrated data obtained for the complexation of selected glycoassemblies with Con A at 25 °C, and the results of all ITC studies are summarized in Table 1. The dissociation constant (K_d) for the binding of $[NMe_4]_4[1e]$ with Con A was determined to be $5.18\pm0.51 \,\mu\text{M}$, reflecting a nearly 20-fold enhancement compared to the that of monovalent, methyl α -D-mannopyranoside. [50,72,79] This binding enhancement is attributed to the multivalent nature of these interactions and is consistent with the cluster glycoside effect.^[5,80,81] Notably, the impact of integrating a longer and more flexible linker was evident in the behavior of assembly [1f]⁴⁻, which exhibited an even higher, 40-fold increase in binding affinity for Con A $(K_d = 2.51 \pm 0.25 \,\mu\text{M})$ when

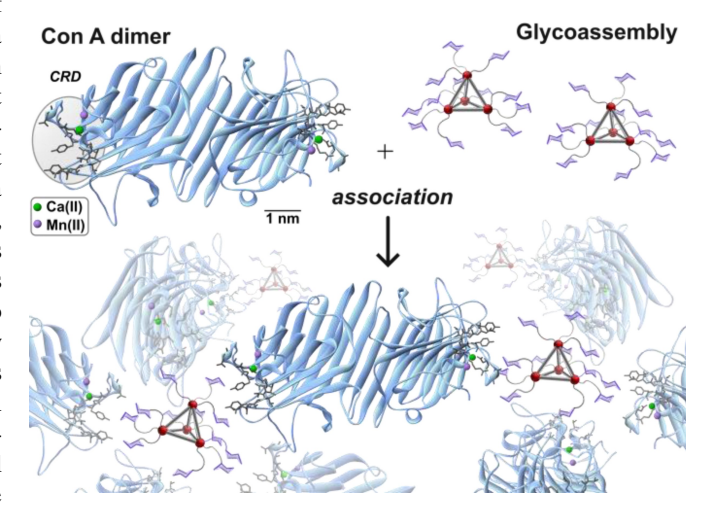


Figure 4. Schematic representation of glycoassembly complexation to Con A (PDB code 1QDC) with the carbohydrate recognition domain (CRD) indicated. Glycoassembly scale approximated based on crystallographically determined structural parameters of the cage core.[44]



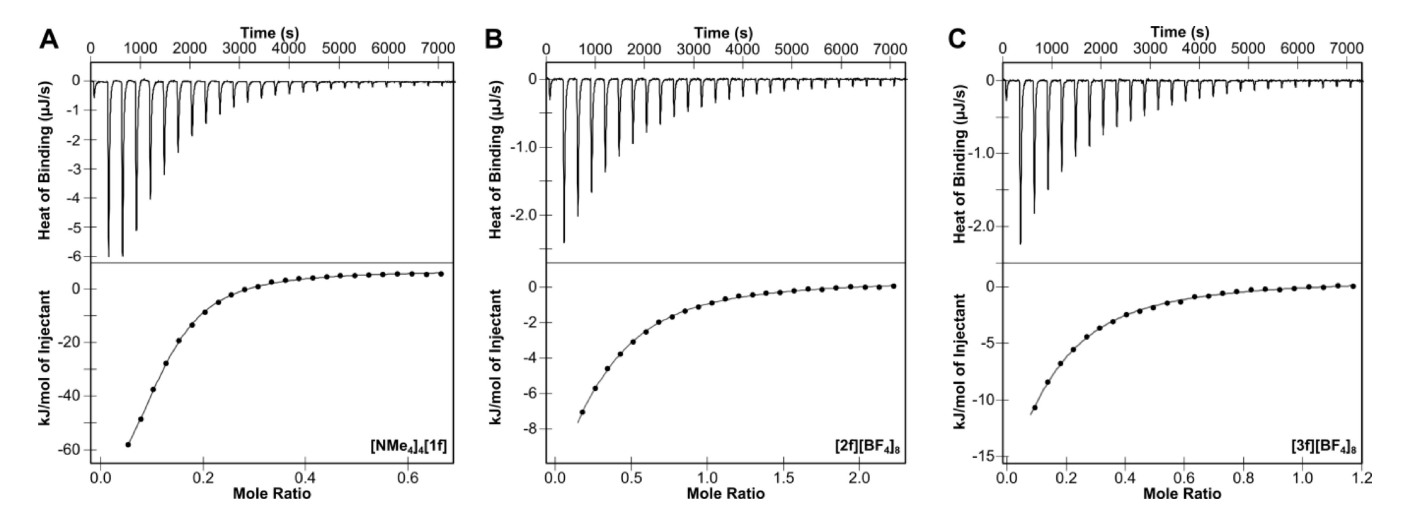


Figure 5. ITC thermograms (top) and fitted binding isotherms (bottom) for the binding of selected assemblies based on subcomponent f to dimeric Con A: $[NMe_4]_4[1 f]$ (A), $[2 f][BF_4]_8$ (B), and $[3 f][BF_4]_8$ (C).

compared to the binding of monovalent methyl a-Dmannopyranoside. A direct comparison of the K_d values of the two glycoassemblies reveals that [1f]4- displays a twofold higher binding affinity for Con A than [1e]4-. Furthermore, [1f]⁴⁻ also demonstrates a 24 kJ/mol increase in enthalpic contribution ($\Delta H = -91.03 \pm 4.09 \text{ kJ/mol}$) for this macromolecular interaction relative to that of first-generation $[1e]^{4-}$ ($\Delta H = -59.95 \pm 4.09 \text{ kJ/mol}$), which agrees well with its stronger binding strength.

The incorporation of an additional ethylene glycol unit as represented in assembly $[1g]^{4-}$ again led to an increase in affinity when compared to the binding of the parent $[1e]^{4-}$ assembly. However, the additional EG group did not significantly alter the binding strength when compared to that of [1f]4-, and in fact resulted in a modest decrease in affinity ($K_d = 3.15 \pm 0.27 \,\mu\text{M}$). Furthermore, introduction of a third EG unit resulted in a more pronounced decrease in binding strength relative to that of $[1f]^{4-}$, as reflected in the K_d value of $4.32 \pm 0.52 \,\mu\text{M}$ measured for assembly $[1\,\text{h}]^{4-}$ (Table 1). The data presented in Table 1 demonstrate that incorporating flexibility within the ligand framework correlates with an enhancement in glycoassembly binding strength. Notably, $[\mathbf{1g}]^{4-}$ and $[\mathbf{1h}]^{4-}$ exhibit 1.7- and 1.2-fold improvements, respectively, compared to the binding of the first generation $[1e]^{4-}$ assembly, which features the shortest and least flexible connecting chain. These results clearly illustrate that the length and degree of flexibility of the saccharide tether directly influence the affinities of the resultant assemblies for Con A.

Evaluation of the thermodynamic contributions to these binding interactions indicates that [1f]⁴⁻ exhibits the strongest enthalpy of binding, followed by $[1g]^{4-}$, $[1h]^{4-}$, and $[1e]^{4-}$, mirroring the observed trend in K_d values (see above). The incorporation of EG linkages increases the conformational flexibility of $[\mathbf{1f}]^{4-}$, $[\mathbf{1g}]^{4-}$, and $[\mathbf{1h}]^{4-}$, which potentially allows these assemblies to overcome unfavorable steric interactions associated with accessing the Con A binding pocket, consequently leading to stronger interactions and enhanced affinity. These findings suggest that the short chain length of [1e]4- may not provide the assembly with an optimal spatial arrangement of saccharides to most effectively engage with Con A due to their proximity to the rigid cage core.[82]

The binding stoichiometry for the $[1e-h]^{4-}$ series of assemblies with monomeric Con A was determined to be $n_{\rm avg} = 0.11 \pm 0.01$, indicating that each glycoassembly has a functional valence, N(1/n), of nine. These data indicate that that the mannose units of each assembly are positioned sufficiently far apart from each other to accommodate complexation with nine Con A monomers without significant steric interference. This result agrees well with ITCderived binding stoichiometry reported for other multivalent systems, including a similarly-sized octasilsesquioxane glycomolecule that also binds Con A with a functional valence of nine.[30] High N values are commonly observed for denselyfunctionalized multivalent glycan systems, [18,83-85] which aligns well with previous reports indicating that that short mannoside chains can bridge two Con A binding sites and

Table 1: ITC-derived thermodynamic parameters for the $[NMe_4]_4[1]$, $[2][BF_4]_8$, and $[3][BF_4]_8$ series of complexes.

Entry	Glycoassembly	K_{d} [μ M]	$n^{[a]}$	$-\Delta H$ [kJ/mol]
1	[NMe ₄] ₄ [1 e] ^[b]	5.18±0.51	0.11 ± 0.01	59.95 ± 4.09
2	[NMe ₄] ₄ [1 f]	2.51 ± 0.25	0.12 ± 0.01	91.03 ± 4.09
3	[NMe ₄] ₄ [1 g]	3.15 ± 0.27	0.10 ± 0.01	82.31 ± 4.45
4	[NMe ₄] ₄ [1 h]	4.32 ± 0.52	$\textbf{0.11} \pm \textbf{0.01}$	76.67 ± 6.54
5	[2 e][BF ₄] ₈	80.76 ± 1.33	$\boldsymbol{0.39 \pm 0.09}$	14.17 ± 3.50
6	[2 f][BF ₄] ₈	21.88 ± 4.36	0.26 ± 0.04	22.74 ± 5.49
7	[2g][BF ₄] ₈	31.91 ± 5.76	$\boldsymbol{0.20\pm0.07}$	33.75 ± 9.18
8	$[2 h][BF_4]_8$	44.48 ± 8.99	$\textbf{0.18} \pm \textbf{0.05}$	26.40 ± 5.85
9	[3 e][BF ₄] ₈	34.96 ± 7.85	$\boldsymbol{0.32\pm0.06}$	21.70 ± 5.71
10	$[3 f][BF_4]_8$	18.91 ± 2.47	$\boldsymbol{0.19 \pm 0.02}$	58.23 ± 8.51
11	[3 g][BF ₄] ₈	24.69 ± 5.40	0.26 ± 0.05	20.89 ± 5.81
12	[3 h][BF ₄] ₈	27.04 ± 4.65	$\textbf{0.24} \pm \textbf{0.03}$	23.40 ± 3.74

[a] Binding stoichiometry of the glycoassembly/Con A complexation with respect to monomeric Con A. [b] Refs [50] and [79].



allow proteins to approach without making substantial contact. $^{[4,86]}$

Since the separation between dimeric Con A binding sites is too large to enable chelation by the glycoassemblies, the enhanced affinity of [1f-h]⁴⁻ is likely attributed to the heightened flexibility of the EG linkages that facilitate favorable statistical rebinding and cross-linking operating mechanisms that maximize the multivalency effect (Figure 2).^[58] In fact, similar variations in binding behavior have been reported for other multivalent glycoassemblies in which the degree of flexibility of the saccharide linking units modulates the lectin binding strength. [30,55,87-89] Additional experiments using dynamic light scattering (DLS) (see Supporting Information Section S5) also indicated the coexistence of dimeric lectin/single glycoassembly complexes (hydrodynamic diameter $(D_h)=12 \text{ nm}$), and large, soluble oligomeric forms (D_h = ca. 98–383 nm) from the initial stages of the lectin-assembly binding process under experimental conditions mimicking the ITC binding studies. The presence of smaller-sized species supports the statistical rebinding mode of multivalent binding in which the value of 12 nm corresponds to the sum of the Con A dimer and a single glycoassembly, whereas large oligomers provide evidence for a cross-linking multivalent mechanism, [30,72] highlighting the significance of both processes in this dynamic biomolecular recognition event.

Building on these results, we next evaluated the capacity of the cationic [2e-h]⁸⁺ series to engage Con A. The dissociation constant for the binding of [2e]⁸⁺ with Con A was determined to be $80.76 \pm 1.33 \,\mu\text{M}$, which represents a considerable 16-fold reduction in strength when compared to the binding of the tetraanionic analogue, $[1e]^{4-}$. The comparable size and morphology of the two assemblies suggest that the overall charge of the cage plays a pivotal role in the strength of the molecular recognition event. While size and shape contribute to the overall fit within the protein binding site, these results underscore the critical contribution of electrostatic effects in determining the strength of the binding. Such findings provide insights into the nuances of molecular recognition interactions between glycoassemblies and their binding partners and provide valuable information guiding synthetic design.

A consistent trend in binding strength was observed for the $[\mathbf{2e}-\mathbf{h}]^{8+}$ systems as similarly demonstrated by the $[\mathbf{1e}-\mathbf{h}]^{4-}$ series. Specifically, $[\mathbf{2f}]^{8+}$, which features the diethylene glycol linker, displayed the highest binding affinity with Con A $(K_d=21.88\pm4.36~\mu\text{M})$, whereas the parent $[\mathbf{2e}]^{8+}$ complex, which features the least flexible tether, exhibited the weakest binding $(K_d=80.76\pm1.33~\mu\text{M})$. As similarly observed for the $[\mathbf{1e}-\mathbf{h}]^{4-}$ series, assemblies featuring the tri- $([\mathbf{2g}]^{8+}~K_d=31.91\pm5.76~\mu\text{M})$ and tetraethyleneglycol $([\mathbf{2h}]^{8+}~K_d=44.48\pm8.99~\mu\text{M})$ linkers demonstrated the second and third strongest binding, respectively; this consistency further underscores the critical role that the length of the EG linker plays in achieving optimal lectin binding.

Further studies were performed to measure the binding capacity of the second set of cationic complexes ($[3e-g]^{8+}$) with Con A, and Table 1 summarizes the results. The K_d

value determined for the $[3\,\mathrm{e}]^{8+}/\mathrm{Con}\,\mathrm{A}$ interaction was found to be $34.96\pm7.85\,\mu\mathrm{M}$, representing a 7-fold decrease in binding when compared to the K_d value determined for the anionic $[1\,\mathrm{e}]^{4-}$ assembly. These results underscore the notable decrease in strength for assemblies carrying a positive charge when interacting with the protein. For this series, the diethylene glycol linkage again offered the length and flexibility to promote the strongest interaction as evidenced by the K_d value of $18.91\pm2.47\,\mu\mathrm{M}$ for $[3\,\mathrm{f}]^{8+}$, while the binding profiles for the tri- $([3\,\mathrm{g}]^{8+},\,K_\mathrm{d}=24.69\pm5.40\,\mu\mathrm{M})$ and tetraethylene glycol $([3\,\mathrm{h}]^{8+},\,K_\mathrm{d}=27.04\pm4.65\,\mu\mathrm{M})$ derivatives showed comparable results.

The binding data for all series indicate that the incorporation of EG linkages strengthens the overall interactions of the resultant assemblies with Con A. This result is consistent with both statistical rebinding and cross-linking mechanisms of binding as the EG tethers may allow higher local concentrations of glycan units around the binding pocket due to their increased flexibility while also decreasing the steric crowding around the assembly to promote a cross-linking mechanism. There is, however, an optimal chain length that facilitates the strongest multivalent binding. In these series, the diethylene glycol linkages offer multiple functional advantages: they provide the appended saccharides with optimal distance relative to the Fe₄ core and impart the necessary flexibility for the assemblies to engage with and access the protein binding pocket most effectively. Chains of longer length (g, h), however, increase the intersaccharide distances, which consequently reduces the saccharide density at the protein surface. This result comparatively decreases the cluster glycoside effect and weakens the multivalent binding interactions. [90,91]

Contrasting the binding affinities of $[2e]^{8+}$ and $[3e]^{8+}$ illustrates that the slightly larger footprint of $[3e]^{8+}$ positively affects its binding strength. These data underscore that even subtle differences in molecular structure can impact binding properties and suggest that the overall size and shape of $[3e]^{8+}$ may better complement the Con A binding pocket. Interestingly, the binding strength of the diethyleneglycol derivatives, $[3f]^{8+}$ and $[2f]^{8+}$, are comparable, which is likely due to the enhanced flexibility of the diethyleneglycol tether, which allows both systems to adopt similar conformations to optimize interactions with the binding pocket despite their structural differences.

Direct comparison of the K_d values determined for the 1, 2, and 3 series of glycan assemblies demonstrates the cationic 2 and 3 species exhibit significantly weaker binding with Con A. This discrepancy can likely be attributed to electrostatic repulsion between the positively charged complexes and protein binding site. Con A is a member of the C-type lectin family, which is a class of proteins that bind carbohydrates in a Ca²⁺-dependent manner. [92] Like many lectins, Con A also requires a transition metal ion (typically $Mn(II))^{[93]}$ for carbohydrate binding. The presence of both Ca^{2+} and Mn^{2+} in the Carbohydrate Recognition Domain (CRD) of the protein leads to electrostatic repulsion with cationic [2]⁸⁺ and [3]⁸⁺ complexes, whereas the anionic [1]⁴⁻ series benefits from Coulombic attraction with the CRD, likely contributing to the significantly more favorable



interactions observed by ITC measurements. The average functional valence (N) values that were determined for the interaction between both cationic series with Con A were notably lower (N_{avg} for $[2e-h]^{8+}=4$; N_{avg} for $[3e-h]^{8+}=4$) than those calculated for the anionic series (see above). This behavior aligns with the lower binding affinities determined for the $[2e-h]^{8+}$ and $[3e-h]^{8+}$ families of complexes and can be attributed to the electrostatic repulsion between the Con A binding sites and the cationic assemblies. This repulsive effect likely precludes a larger number of proteins from approaching each cationic cage despite the apparent spatial accommodations.

For a metal-dependent lectin like Con A, anionic glycomolecules may provide the strongest binding partners, rendering supramolecular assemblies supported by neutral iminopyridine ligands less desirable. These findings provide valuable insights into structure-function relationships and offer important considerations from a molecular design perspective. Despite these findings, however, we cannot simply exclude neutral subcomponents from the library of organic building blocks used in this platform. There are in fact lectins that regulate a diverse range of biological functions that do not require divalent cations for carbohydrate binding. Galectins, or S-type lectins, are a class of calcium-independent mammalian carbohydrate binding proteins that selectively recognize galactose residues and are involved in varied physiological processes including immune response, cell-cell communication, pathological responses, among others.^[94] The pivotal role lectins play in these processes underscores the importance of understanding how to program multivalent binders that efficiently target such proteins, as these systems hold direct implications in therapeutic applications and may be better suited binding partners for cationic hybrid assemblies.

While a range of neutral glycosylated platforms have been extensively studied to probe saccharide-based multivalent interactions, instances of precisely-defined charged molecular glycan systems remain relatively rare. [26–28,31,50,95] This scarcity has limited systematic investigations into the influence of electrostatic contributions on these complex interactions. This work offers a versatile and unique synthetic platform in which the charge of a glycoassembly can be specifically tuned to complement the electrostatic properties of a protein CRD, which is an element of tunability not accessible with conventional multivalent glycoconjugates.

The introduction of cationic assemblies to this supramolecular platform has potential implications in the biomedical field, including antibiofilm applications. Recently, Vincent et al. reported a series of polycationic pillar[5]arene glycorotaxanes that show strong and selective antibiofilm activity against Gram-negative bacteria through synergistic action of the multivalent presentation of saccharides and the presence of polycationic subunits. [95] These types of studies offer exciting opportunities to leverage the tunable electronic properties of metallosupramolecular glycan assemblies and opens the possibility to employ neutral subcomponents paired with saccharide building

blocks to program functional polycationic nanocages that could potentially serve as a new class of antibiofilm agents.

Conclusion

This work describes efforts to evaluate how structural, topological, and electronic aspects of supramolecular multivalent glycoconjugates influence lectin binding. Examples described here underscore the importance of several aspects of subcomponent design and highlight the considerable potential of this synthetic approach for precisely tailoring the strength of multivalent binding. The comparison of ITCderived K_d values between glycoassemblies bearing systematically varied EG chain lengths demonstrates the importance of achieving optimal intersaccharide distance and epitope spatial arrangements. Binding data revealed that glycocomplexes featuring diethyleneglycol chains provided the ideal length and flexibility of tethered peripheral saccharide units, offering valuable structural insights for optimizing carbohydrate presentation. Additionally, the significantly diminished binding observed for the two sets of cationic assemblies compared to their anionic counterparts introduces valuable design considerations that highlight the importance of electrostatic contributions on protein recognition. Synthetic control over the electronics of glycan assemblies provides another element of ligand design at our disposal that can be adjusted to complement the unique chemical environments of lectin receptors. This work contributes to the broader understanding of glycan-protein interactions at the fundamental molecular level and opens avenues for the design of "custom-built" systems that can potentially be tailored to specific protein binding partners. The operational simplicity and flexibility of this synthetic approach position it favorably for further exploration and advances progress towards harnessing the potential of supramolecular coordination complexes as functional materials with biomedical applications. $\hat{s}_{1,42,95-100}$

Supporting Information

The data that support the findings of this study are available in the supplementary material of the article. The ESI contains synthetic details, spectroscopic and analytical data of all compounds, and ITC binding studies.

Acknowledgements

This work was supported by UCSD startup funds and sponsored in part by the UC San Diego Materials Research Science and Engineering Center (UCSD MRSEC), supported by the National Science Foundation (NSF) (DMR-2011924). Shawn McClure is thanked for performing DLS measurements and Ricardo De Luna (UCSD MRSEC Materials Characterization Facility) is thanked for help conducting these measurements.

Conflict of Interest

The authors declare no conflict of interest.

Data Availability Statement

The data that support the findings of this study are available in the supplementary material of this article.

Keywords: glycoconjugates · molecular recognition · multivalent binding · self-assembly · supramolecular chemistry

- [1] O. Konur, Glycoscience, CRC Press, Boca Raton, 2016.
- [2] R. Das, B. Mukhopadhyay, Carbohydr. Res. 2021, 507, 108394.
- [3] M. Mammen, S.-K. Choi, G. M. Whitesides, Angew. Chem. Int. Ed. 1998, 37, 2454–2794.
- [4] S. M. Dimick, S. C. Powell, S. A. McMahon, D. N. Moothoo, J. H. Naismith, E. J. Toone, J. Am. Chem. Soc. 1999, 121, 10286–10296.
- [5] C. Müller, G. Despras, T. K. Lindhorst, Chem. Soc. Rev. 2016, 45, 3275–3302.
- [6] C. Fasting, C. A. Schalley, M. Weber, O. Seitz, S. Hecht, B. Koksch, J. Dernedde, C. Graf, E.-W. Knapp, R. Haag, Angew. Chem. Int. Ed. 2012, 51, 10472–10498.
- [7] A. K. Bakshi, T. Haider, R. Tiwari, V. Soni, *Drug Delivery Transl. Res.* 2022, 12, 2335–2358.
- [8] M. González-Cuesta, C. Ortiz Mellet, J. M. García Fernández, Chem. Commun. 2020, 56, 5207–5222.
- [9] J. Rojo, J. C. Morales, S. Penadés, *Top. Curr. Chem.* 2010, 218.
- [10] M. Touaibia, T. C. Shiao, A. Papadopoulos, J. Vaucher, Q. Wang, K. Benhamioud, R. Roy, Chem. Commun. 2007, 16, 380, 382
- [11] A. Dondoni, A. Marra, Chem. Rev. 2010, 110, 4949–4977.
- [12] S. J. L. Petitjean, W. Chen, M. Koehler, R. Jimmidi, J. Yang, D. Mohammed, B. Juniku, M. L. Stanifer, S. Boulant, S. P. Vincent, D. Alsteens, *Nat. Commun.* 2022, 13, 1–12.
- [13] S. Sakai, T. Sasaki, J. Am. Chem. Soc. 1994, 116, 1587–1588.
- [14] J. A. D. MacKerell, B. Brooks, I. C. L. Brooks, L. Nilsson, B. Roux, Y. Won, M. Karplus, in *Encycl. Comput. Chem.* (Ed.: P. v. R. S. et al.), John Wiley & Sons: Chichester, 1998, pp. 271–277.
- [15] V. Percec, P. Leowanawat, H.-J. Sun, O. Kulikov, C. D. Nusbaum, T. M. Tran, A. Bertin, D. A. Wilson, M. Peterca, S. Zhang, N. P. Kamat, K. Vargo, D. Moock, E. D. Johnston, D. A. Hammer, D. J. Pochan, Y. Chen, Y. M. Chabre, T. C. Shiao, M. Bergeron-Brlek, S. André, R. Roy, H.-J. Gabius, P. A. Heiney, J. Am. Chem. Soc. 2013, 135, 9055–9077.
- [16] C. W. Cairo, J. E. Gestwicki, M. Kanai, L. L. Kiessling, J. Am. Chem. Soc. 2002, 124, 1615–1619.
- [17] K. Godula, C. R. Bertozzi, J. Am. Chem. Soc. 2010, 132, 9963–9965.
- [18] R. S. Loka, M. S. McConnell, H. M. Nguyen, *Biomacromole-cules* 2015, 16, 4013–4021.
- [19] M. C. Galan, P. Dumy, O. Renaudet, Chem. Soc. Rev. 2013, 42, 4599–4612.
- [20] I. S. MacPherson, J. S. Temme, S. Habeshian, K. Felczak, K. Pankiewicz, L. Hedstrom, I. J. Krauss, *Angew. Chem. Int. Ed.* 2011, 50, 11238–11242.
- [21] M. Ciobanu, K. T. Huang, J. P. Daguer, S. Barluenga, O. Chaloin, E. Schaeffer, C. G. Mueller, D. A. Mitchell, N. Winssinger, *Chem. Commun.* 2011, 47, 9321–9323.

- [22] M. Marradi, F. Chiodo, I. García, S. Penadés, *Chem. Soc. Rev.* 2013, 42, 4728–4745.
- [23] B. K. Gorityala, J. Ma, X. Wang, P. Chen, X. W. Liu, Chem. Soc. Rev. 2010, 39, 2925–2934.
- [24] A. Muñoz, D. Sigwalt, B. M. Illescas, J. Luczkowiak, L. Rodríguez-Pérez, I. Nierengarten, M. Holler, J. S. Remy, K. Buffet, S. P. Vincent, J. Rojo, R. Delgado, J. F. Nierengarten, N. Martín, *Nat. Chem.* 2016, 8, 50–57.
- [25] F. Osaki, T. Kanamori, S. Sando, T. Sera, Y. Aoyama, J. Am. Chem. Soc. 2004, 126, 6520–6521.
- [26] N. Kamiya, M. Tominaga, S. Sato, M. Fujita, J. Am. Chem. Soc. 2007, 129, 3816–3817.
- [27] F. Zhou, S. Li, T. R. Cook, Z. He, P. J. Stang, Organometallics 2014, 33, 7019–7022.
- [28] E. A. Qian, A. I. Wixtrom, J. C. Axtell, A. Saebi, D. Jung, P. Rehak, Y. Han, E. H. Moully, D. Mosallaei, S. Chow, M. S. Messina, J. Y. Wang, A. T. Royappa, A. L. Rheingold, H. D. Maynard, P. Král, A. M. Spokoyny, *Nat. Chem.* 2017, 9, 333–340
- [29] M. J. Chmielewski, E. Buhler, J. Candau, J. Lehn, *Chem. A Eur. J.* 2014, 20, 6960–6977.
- [30] B. Trastoy, D. A. Bonsor, M. E. Pérez-Ojeda, M. L. Jimeno, A. Méndez-Ardoy, J. M. García Fernández, E. J. Sundberg, J. L. Chiara, Adv. Funct. Mater. 2012, 22, 3191–3201.
- [31] C. Pritchard, M. Ligorio, G. D. Jackson, M. I. Gibson, M. D. Ward, ACS Appl. Mater. Interfaces 2023, 15, 36052–36060.
- [32] R. Ham, C. J. Nielsen, S. Pullen, J. N. H. Reek, *Chem. Rev.* 2023, 123, 5225–5261.
- [33] M. D. Ward, P. R. Raithby, Chem. Soc. Rev. 2013, 42, 1619– 1636.
- [34] M. M. Conn, J. Rebek, Chem. Rev. 1997, 97, 1647-1668.
- [35] R. Chakrabarty, P. S. Mukherjee, P. J. Stang, Chem. Rev. 2011, 111, 6810–6918.
- [36] T. R. Cook, P. J. Stang, Chem. Rev. 2015, 115, 7001-7045.
- [37] R. Saha, B. Mondal, P. S. Mukherjee, Chem. Rev. 2022, 122, 12244–12307.
- [38] Z. J. Wang, K. N. Clary, R. G. Bergman, K. N. Raymond, F. D. Toste, *Nat. Chem.* 2013, 5, 100–103.
- [39] W. Cullen, A. J. Metherell, A. B. Wragg, C. G. P. Taylor, N. H. Williams, M. D. Ward, J. Am. Chem. Soc. 2018, 140, 2821–2828.
- [40] N. Ahmad, H. A. Younus, A. H. Chughtai, F. Verpoort, Chem. Soc. Rev. 2015, 44, 9–25.
- [41] T. R. Cook, V. Vajpayee, M. H. Lee, P. J. Stang, K. W. Chi, Acc. Chem. Res. 2013, 46, 2464–2474.
- [42] A. Casini, B. Woods, M. Wenzel, *Inorg. Chem.* 2017, 56, 14715–14729.
- [43] A. Brzechwa-Chodzyńska, W. Drożdż, J. Harrowfield, A. R. Stefankiewicz, Coord. Chem. Rev. 2021, 434, 213820.
- [44] P. Mal, B. Breiner, K. Rissanen, J. R. Nitschke, Science 2009, 324, 1697–1700.
- [45] J. Roukala, J. Zhu, C. Giri, K. Rissanen, P. Lantto, V. V. Telkki, J. Am. Chem. Soc. 2015, 137, 2464–2467.
- [46] D. M. Vriezema, M. C. Aragonès, J. A. A. W. Elemans, J. J. L. M. Cornelissen, A. E. Rowan, R. J. M. Nolte, *Chem. Rev.* 2005, 105, 1445–1489.
- [47] D. Fujita, K. Suzuki, S. Sato, M. Yagi-Utsumi, Y. Yamaguchi, N. Mizuno, T. Kumasaka, M. Takata, M. Noda, S. Uchiyama, K. Kato, M. Fujita, *Nat. Commun.* 2012, 3, 1093–1097.
- [48] H. Vardhan, M. Yusubov, F. Verpoort, Coord. Chem. Rev. 2016, 306, 171–194.
- [49] A. V. Virovets, E. Peresypkina, M. Scheer, Chem. Rev. 2021, 121, 14485–14554.
- [50] J. H. Schwab, J. B. Bailey, M. Gembicky, J. M. Stauber, Chem. Sci. 2023, 14, 1018–1026.
- [51] S. Zarra, J. K. Clegg, J. R. Nitschke, Angew. Chem. Int. Ed. 2013, 52, 4837–4840.



- [52] L. Fabbrizzi, J. Org. Chem. 2020, 85, 12212-12226.
- [53] J. L. Bolliger, A. M. Belenguer, J. R. Nitschke, Angew. Chem. Int. Ed. 2013, 52, 7958–7962.
- [54] K. Marotte, C. Préville, C. Sabin, M. Moumé-Pymbock, A. Imberty, R. Roy, Org. Biomol. Chem. 2007, 5, 2953–2961.
- [55] D. Deniaud, K. Julienne, S. G. Gouin, *Org. Biomol. Chem.* 2011, 9, 966–979.
- [56] A. A. D'souza, R. Shegokar, Expert Opin. Drug Delivery 2016, 13, 1257–1275.
- [57] M. Duca, D. Haksar, J. van Neer, D. M. E. Thies-Weesie, D. Martínez-Alarcón, H. de Cock, A. Varrot, R. J. Pieters, ACS Chem. Biol. 2022, 17, 3515–3526.
- [58] R. J. Pieters, Org. Biomol. Chem. 2009, 7, 2013.
- [59] Z. Wang, in Compr. Org. Name React. Reagents, John Wiley & Sons, Inc., Hoboken, NJ, 2010, pp. 3123–3128.
- [60] R. A. Bilbeisi, J. K. Clegg, N. Elgrishi, X. de Hatten, M. Devillard, B. Breiner, P. Mal, J. R. Nitschke, J. Am. Chem. Soc. 2012, 134, 5110–5119.
- [61] J. K. Clegg, J. C. McMurtrie, in *Chirality Supramol. Assem.* (Ed.: F. R. Keene), Wiley-VCH, Weinheim, 2016, pp. 218–256.
- [62] T. F. Miller, L. R. Holloway, P. P. Nye, Y. Lyon, G. J. O. Beran, W. H. Harman, R. R. Julian, R. J. Hooley, *Inorg. Chem.* 2018, 57, 13386–13396.
- [63] A. M. McDaniel, A. K. Rappé, M. P. Shores, *Inorg. Chem.* 2012, 51, 12493–12502.
- [64] P. Mal, D. Schultz, K. Beyeh, K. Rissanen, J. R. Nitschke, Angew. Chem. Int. Ed. 2008, 47, 8297–8301.
- [65] W. F. Baitinger, P. V. R. Schleyer, K. Mislow, J. Am. Chem. Soc. 1965, 87, 3168–3173.
- [66] D. Casarini, L. Lunazzi, M. Mancinelli, A. Mazzanti, C. Rosini, J. Org. Chem. 2007, 72, 7667–7676.
- [67] R. Ruzziconi, S. Spizzichino, A. Mazzanti, L. Lunazzi, M. Schlosser, Org. Biomol. Chem. 2010, 8, 4463–4471.
- [68] G. Argouarch, R. Veillard, T. Roisnel, A. Amar, H. Meghezzi, A. Boucekkine, V. Hugues, O. Mongin, M. Blanchard-Desce, F. Paul, Chem. A Eur. J. 2012, 18, 11811–11827
- [69] B. Roy, E. Zangrando, P. S. Mukherjee, Chem. Commun. 2016, 52, 4489–4492.
- [70] E. G. Percástegui, T. K. Ronson, J. R. Nitschke, Chem. Rev. 2020, 120, 13480–13544.
- [71] M. Whitehead, S. Turega, A. Stephenson, C. A. Hunter, M. D. Ward, *Chem. Sci.* 2013, 4, 2744–2751.
- [72] T. K. Dam, R. Roy, S. K. Das, S. Oscarson, C. F. Brewer, J. Biol. Chem. 2000, 275, 14223–14230.
- [73] T. K. Dam, C. F. Brewer, Chem. Rev. 2002, 102, 387-429.
- [74] R. Katoch, A. Tripathi, J. Biosci. 2021, 46.
- [75] H. Lis, N. Sharon, Chem. Rev. 1998, 98, 637-674.
- [76] H. Kogelberg, T. Feizi, Curr. Opin. Struct. Biol. 2001, 11, 635–643.
- [77] Z. Derewenda, J. Yariv, J. R. Helliwell, A. J. Kalb, E. J. Dodson, M. Z. Papiz, T. Wan, J. Campbell, *EMBO J.* **1989**, 8, 2189–2193.
- [78] M. L. Wolfenden, M. J. Cloninger, J. Am. Chem. Soc. 2005, 127, 12168–12169.
- [79] We previously reported ITC-derived thermodynamic data for the binding of [NMe₄]₄[1e] with Con A^[50] and have since recollected data sets with a different instrument using different titrant and protein concentrations. These experiments provided higher quality data with improved levels of reproducibility, and the improved data are reported in this work.

- [80] J. J. Lundquist, E. J. Toone, Chem. Rev. 2002, 102, 555-578.
- [81] R. T. Lee, Y. C. Lee, Glycoconjugate J. 2000, 17, 543–551.
- [82] W. Jeong, J. Bu, R. Jafari, P. Rehak, L. J. Kubiatowicz, A. J. Drelich, R. H. Owen, A. Nair, P. A. Rawding, M. J. Poellmann, C. M. Hopkins, P. Král, S. Hong, Adv. Sci. 2022, 9, 1–11.
- [83] S. H. Liyanage, M. Yan, Chem. Commun. 2020, 56, 13491– 13505.
- [84] M. Nagao, M. Kichize, Y. Hoshino, Y. Miura, *Biomacromole-cules* 2021, 22, 3119–3127.
- [85] Z. Liu, Y. Zhu, W. Ye, T. Wu, D. Miao, W. Deng, M. Liu, Polym. Chem. 2019, 10, 4006–4016.
- [86] M. François-Heude, A. Méndez-Ardoy, V. Cendret, P. Lafite, R. Daniellou, C. O. Mellet, J. M. García Fernández, V. Moreau, F. Djedaïni-Pilard, *Chem. A Eur. J.* 2015, 21, 1978–1991.
- [87] T. K. Dam, S. Oscarson, R. Roy, S. K. Das, D. Pagé, F. Macaluso, C. F. Brewer, J. Biol. Chem. 2005, 280, 8640–8646.
- [88] S. Cecioni, J. P. Praly, S. E. Matthews, M. Wimmerová, A. Imberty, S. Vidal, *Chem. A Eur. J.* 2012, 18, 6250–6263.
- [89] B. N. Murthy, S. Sinha, A. Surolia, S. S. Indi, N. Jayaraman, Glycoconjugate J. 2008, 25, 313–321.
- [90] V. Bandlow, S. Liese, D. Lauster, K. Ludwig, R. R. Netz, A. Herrmann, O. Seitz, J. Am. Chem. Soc. 2017, 139, 16389– 16397.
- [91] D. Lauster, S. Klenk, K. Ludwig, S. Nojoumi, S. Behren, L. Adam, M. Stadtmüller, S. Saenger, S. Zimmler, K. Hönzke, L. Yao, U. Hoffmann, M. Bardua, A. Hamann, M. Witzenrath, L. E. Sander, T. Wolff, A. C. Hocke, S. Hippenstiel, S. De Carlo, J. Neudecker, K. Osterrieder, N. Budisa, R. R. Netz, C. Böttcher, S. Liese, A. Herrmann, C. P. R. Hackenberger, Nat. Nanotechnol. 2020, 15, 373–379.
- [92] G. D. Brown, J. A. Willment, L. Whitehead, Nat. Rev. Immunol. 2018, 18, 374–389.
- [93] S. Kaushik, D. Mohanty, A. Surolia, Biophys. J. 2009, 96, 21– 34
- [94] A. Radhakrishnan, H. Chellapandian, P. Ramasamy, S. Jeyachandran, J. Proteins Proteomics 2022, 14, 43–59.
- [95] T. Mohy El Dine, R. Jimmidi, A. Diaconu, M. Fransolet, C. Michiels, J. De Winter, E. Gillon, A. Imberty, T. Coenye, S. P. Vincent, J. Med. Chem. 2021, 64, 14728–14744.
- [96] Y. P. Wang, Y. Zhang, X. H. Duan, J. J. Mao, M. Pan, J. Shen, C. Y. Su, Coord. Chem. Rev. 2024, 501, 215570.
- [97] B. Woods, R. D. M. Silva, C. Schmidt, D. Wragg, M. Cavaco, V. Neves, V. F. C. Ferreira, L. Gano, T. S. Morais, F. Mendes, J. D. G. Correia, A. Casini, *Bioconjugate Chem.* 2021, 32, 1399–1408.
- [98] S. Bhattacharyya, M. Venkateswarulu, J. Sahoo, E. Zangrando, M. De, P. S. Mukherjee, *Inorg. Chem.* 2020, 59, 12690–12699.
- [99] H. Sepehrpour, W. Fu, Y. Sun, P. J. Stang, J. Am. Chem. Soc. 2019, 141, 14005–14020.
- [100] B. P. Burke, W. Grantham, M. J. Burke, G. S. Nichol, D. Roberts, I. Renard, R. Hargreaves, C. Cawthorne, S. J. Archibald, P. J. Lusby, J. Am. Chem. Soc. 2018, 140, 16877–16881.

Manuscript received: May 8, 2024 Accepted manuscript online: June 3, 2024 Version of record online: ••, ••

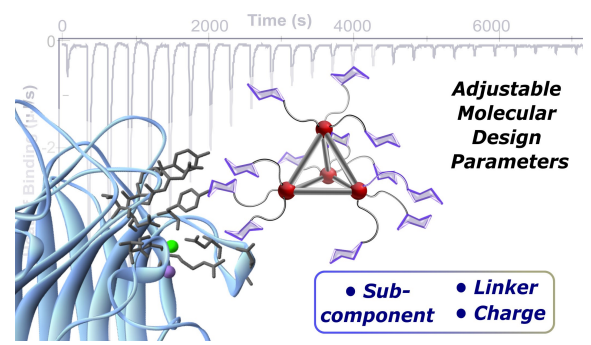
Research Article

Research Article

Molecular Recognition

J. M. Stauber* ______ e202408751

Tailoring Metallosupramolecular Glycoassemblies for Enhancing Lectin Recognition



A supramolecular approach to the design of structurally precise glyconanoassemblies that leverages the versatility, tunability and modularity of subcomponent self-assembly is described. Structural and electronic changes in ligand

architecture enable a systematic method for understanding intricate structure—activity relationships governing multivalent lectin binding, thus offering insights into optimizing molecular recognition through synthetic design.

15213733 a) Dewnloaded from https://onlinelibrary.wiley.com/doi/10.1002/anic.202408731 by University Of California, Wiley Online Library for rules of use; OA articles are governed by the applicable Creative Commons. License and Conditions, wiley.com/terms-and-conditions) on Wiley Online Library for rules of use; OA articles are governed by the applicable Creative Commons. License and Conditions (https://onlinelibrary.wiley.com/terms-and-conditions) on Wiley Online Library for rules of use; OA articles are governed by the applicable Creative Commons. License and Conditions (https://onlinelibrary.wiley.com/terms-and-conditions) on Wiley Online Library for rules of use; OA articles are governed by the applicable Creative Commons. License and Conditions (https://onlinelibrary.wiley.com/terms-and-conditions) on Wiley Online Library for rules of use; OA articles are governed by the applicable Creative Commons. License and Conditions (https://onlinelibrary.wiley.com/terms-and-conditions) on Wiley Online Library for rules of use; OA articles are governed by the applicable Creative Commons. License and Conditions (https://onlinelibrary.wiley.com/terms-and-conditions) on Wiley Online Library for rules of use; OA articles are governed by the applicable Creative Commons. License and Conditions (https://onlinelibrary.wiley.com/terms-and-conditions) on Wiley Online Library for rules of use; OA articles are governed by the applicable Creative Commons.